

Revisiting Adversarial Attacks on Graph Neural Networks for Graph Classification

Beini Xie*, Heng Chang*, Xin Wang, Tian Bian, Shiji Zhou, Daixin Wang, Zhiqiang Zhang, and Wenwu Zhu, *Fellow, IEEE*

Abstract—Graph neural networks (GNNs) have achieved tremendous success in the task of graph classification and diverse downstream real-world applications. Despite their success, existing approaches are either limited to structure attacks or restricted to local information. This calls for a more general attack framework on graph classification, which faces significant challenges due to the complexity of generating *local-node-level* adversarial examples using the *global-graph-level* information. To address this “global-to-local” problem, we present a general framework *CAMA* to generate adversarial examples by manipulating graph structure and node features in a hierarchical style. Specifically, we make use of Graph Class Activation Mapping and its variant to produce node-level importance corresponding to the graph classification task. Then through a heuristic design of algorithms, we can perform both feature and structure attacks under unnoticeable perturbation budgets with the help of both node-level and subgraph-level importance. Experiments towards attacking four state-of-the-art graph classification models on six real-world benchmarks verify the flexibility and effectiveness of our framework.

Index Terms—Adversarial attack, deep graph learning, graph neural networks, graph classification.

1 INTRODUCTION

GRAPH structured data is ubiquitous for modeling relations and interactions at the level of node classification [1], edge prediction [2], and graph classification [4]. Among them, graph classification plays a vital role in a wide range of domains [3]. For instance, in social network analysis, fake news detection could be treated as a binary graph classification problem on Twitter’s news propagation networks [6]. As powerful tools that illustrate the expressive capability of deep learning on graphs, the family of Graph Neural Networks (GNNs) has gained tremendous popularity over the past few years in graph classification and downstream real-world applications [7], [8], [9].

Despite the powerful ability of GNNs for graph representation learning, their vulnerability to potentially existing adversarial examples on graph-structured data has been revealed recently [10]. This lack of robustness of GNNs would be exploited by fraudsters and spammers and provoke dissent on their applications in security-critical domains. For example, deliberately modified personal identity information will cause credit card fraud [11]. Same as the utilization of graph-structured data, adversarial attacks on

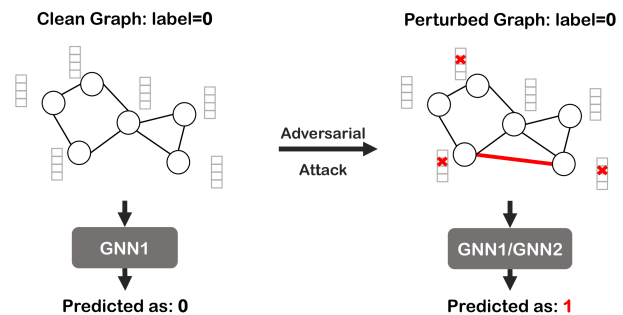


Fig. 1: **Adversarial attack on graph classification.** Given a cleaned graph, we can manipulate node features and edges to generate a poisoned graph to fool the victim GNN.

graphs could also be broadly categorized as node and graph level following the type of tasks. Studies towards node-level adversarial attacks are quite comprehensive from various perspectives [12], [13], [14], [15], [16]. However, in contrast to the remarkable and relatively mature framework for adversarial attacks on node-focused tasks, systematic research and general attacking framework for adversarial attacks on graph classification are still lacking regardless of its vast importance.

Compared with perturbations for node-level classification, migrating these adversarial examples to graph-level tasks is a non-trivial problem, since they have different goals for optimization from local to global scale. A desired attack framework towards graph classification should be general to conduct both feature and structure attack. Moreover, the effective attack on one graph classification model is expected to be able to successfully transferred to other graph classifiers (an illustration can be noticed from Figure 1). In a nutshell, researches on graph classification adversarial attacks still face **three main challenges**:

- * The two first authors made equal contributions.
- B. Xie, H. Chang, S. Zhou are with the Tsinghua-Berkeley Shenzhen Institute, Tsinghua University, Beijing 100084, China. E-mail: {xbn20, changh17, zsj17}@mails.tsinghua.edu.cn
- T. Bian is with the System Engineering and System Management Department, Chinese University of Hong Kong, Hong Kong 999077, China. E-mail: tianbian@link.cuhk.edu.hk
- D. Wang and Z. Zhang are with the Ant Group, Hangzhou 310063, China. E-mail: {daixin.wdx, lingyao.zzq}@antgroup.com
- X. Wang and W. Zhu are with the Department of Computer Science and Technology, Tsinghua University, Beijing 100084, China. E-mail: xin_wang@tsinghua.edu.cn, wwzhu@tsinghua.edu.cn

This work is supported by the National Key Research and Development Program of China No. 2020AAA0106300 and National Natural Science Foundation of China No. 62102222. (Corresponding author: Xin Wang and Wenwu Zhu.)

- Given that graph classification tasks depend on efficiently learning global graph representation from local node embeddings via pooling functions, it is complex to exploit information of global-graph-level classification to generate local-node-level adversarial examples;
- Most current approaches could only attack graph structure. However, node features might contain more fruitful information. For example, personal identity information and loan history apparently matter more in credit models and fraud detection. Thus for a more realistic and practical condition, we need a general attack framework that could both manipulate node features and graph structure;
- Existing attack methods for graph classification using gradient information only consider the training of target models and could not reflect the information from the global graph structure, which might easily result in the generated adversarial edges trapped around a single node as we observe from experiments. Methods with black-box optimization algorithms like reinforcement algorithms or bayesian optimization algorithms suffer the time complexity issue.

To tackle these challenges, we propose a novel hierarchical framework, namely *CAMA*, to bridge the gap between local-node-level and global-graph-level information. We migrate the idea from **Class Activation Mapping (CAM)** [18] to conduct powerful adversarial **Attack** towards graph classification tasks. This unified solution sheds light on the problem of quantifying the contribution of local node information to global representation in attacking graph classification tasks. An example of *CAMA* is shown in Figure 2. Summarizing above, the **main contributions** of our work are outlined below:

- **Framework:** We propose a framework *CAMA* for adversarial attacks on graph classification by hierarchically decomposing the attack process in two steps. Our attack approach fills the gap in generating local perturbation examples from global graph classification. Given the simplicity and effectiveness, *CAMA* can serve as a strong benchmark for future works in this branch.
- **Algorithm:** We heuristically design novel algorithms to select target nodes in a graph by graph class activation mapping and its variant, then generate adversarial examples in the level of both structure and feature.
- **Experiment:** We show that our method could deteriorate graph classification performance by a significant margin on various benchmarks targeting multiple SOTA GNNs. Further, except for white-box attacks, we also test the transferability of our attack method under the black-box setting for evasion attacks.

2 RELATED WORK

GNNs on graph classification. GNNs have proliferate in recent years for tasks like node classification, link prediction, graph classification, and graph generation. GNNs often stack multiple graph convolutions followed by a readout operation to aggregate nodes’ information to a graph-level representation when dealing with graph classification tasks.

Various graph convolution layers and graph pooling operations are proposed to learn both nodes and graph

representation better [19], [22]. One of the most popular GNNs is Graph Convolutional Networks (GCN) [1] which is inspired by the first-order approximation of Chebyshev polynomials in ChebNet. It updates the node representation by taking an average representation of their one-hop neighbors. GCN has excellent results in the semi-supervised node classification tasks. Graph Isomorphism Network (GIN) [23] uses sum aggregation and multi-layer perceptrons instead of one single activation function. It has excellent discriminative power equal to that of the WL test. Facing the finite nature of recurrent GNNs, Implicit Graph Neural Network (IGNN) [24] is able to capture long-range dependencies and performs well in both graph classification and node classification on heterogeneous networks. Its framework ensures well-posedness based on Perron-Frobenius theory.

Except for novel graph convolution operations, diverse pooling strategies affect graph tasks differently. Direct pooling methods like simple node pooling (node-wise mean-pooling, sum-pooling, and max-pooling) directly generate graph-level representation based on node representations [25]. In contrast, hierarchical graph pooling exploits the hierarchical graph structure. DiffPool [26] proposes a differentiable hierarchical clustering algorithm to learn representations of the new coarsened graph by training a soft cluster assign matrix in each layer. Based on graph Fourier transform, EigenPooling [27] jointly uses node features and local structure. The graph pooling layer (gPool) [28] conducts down-sampling on graph data by selecting top-k nodes from calculated projection value. Inversely, the graph unpooling layer (gUnpool) does up-sampling to restore graphs to their original structure. Inspired by U-Net in computer vision, graph U-Nets (g-U-Nets) [28] is proposed using gPool and gUnpooling operations. g-U-Nets can encode and decode high-level features for network embedding.

In this paper, we use GCN, GIN, and IGNN as representatives of general graph classification neural networks and use g-U-Nets to represent hierarchical graph classification models.

Adversarial attacks on graph classification. GNNs have shown their vulnerability under adversarial attacks [29]. Most recent works aim to attack models on node classification tasks [20], [31], [14], [21]. Despite their fruitful progress, these methods can only perform attacks on node-level tasks.

For graph-level tasks, based on reinforcement learning, *RL-S2V* [13] flips edges by selecting two endpoints under black-box attack. *ReWatt* [32] proposes to perform unnoticeable attacks via rewiring operation and utilizes a similar reinforcement learning strategy as *RL-S2V*. *Grabnet* [33] exploits bayesian optimization to conduct adversarial attacks targeting graph classification models. Under the white-box setting, *GradArgmax* [13] exploits gradients over the adjacency matrix of classification loss and flips edges with the largest absolute gradient. *Projective ranking* [34] generates adversarial examples by ranking potential edge perturbation masks through encoding node features and projecting selected edge masks.

Nevertheless, above methods cannot perturb node features. Further, [35] proposes an attacking strategy on hierarchical graph pooling neural networks. However, they overlook the importance of direct pooling, like simple node pooling. Thus, this approach loses its strength when the

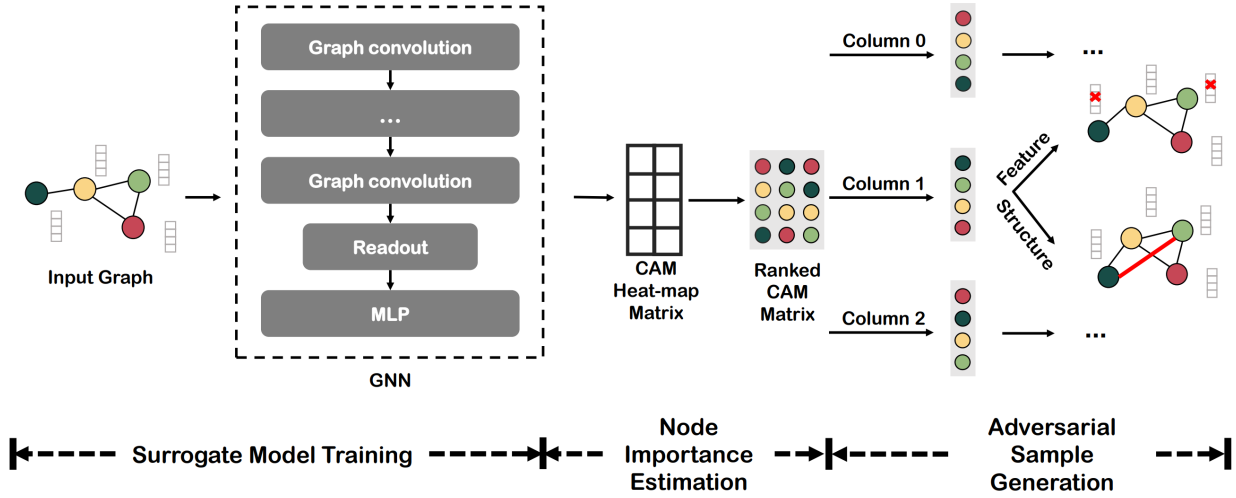


Fig. 2: An example of CAMA for a two-classes graph classification task. After getting the ranked CAM matrix, we select nodes and edges from top-ranked nodes and generate corresponding perturbed graphs. The nodes and edges selection process repeat for each column of the ranked CAM matrix until a successful attack .

graph classification model is unknown. A novel generic attack framework *GraphAttacker* is recently proposed by [36], which could attack on multiple tasks. But the time complexity serves as its main concern due to the process of training the GAN-based model.

Considering all of these, adversarial attacks on graph classification are not fully explored by previous studies. To mitigate this gap, our proposed general framework could flexibly perform structure attack and feature attack. Besides, aside from the white-box attack, we also analyze the transferability of our method under black-box attacks.

CAM on graphs. Class Activation Mapping (CAM) localizes image-level classification into pixel-level image areas by using global average pooling (GAP) in convolutional neural networks in computer vision when it was firstly proposed [37]. CAM has a strong discriminative localization ability in the explanation of image classification. For example, it can localize the toothbrush region in a picture classified as brushing teeth. Compared with the blossom of grand application in computer vision, the utilization of CAM on graph-structured data (Graph CAM) is quite rare with only being applied to the explainability in GNNs [18], [38]. Given a graph classification task, Graph CAM can localize the most influential nodes for classification, which then helps us better understand GNNs. Grad Class Activation Mapping on graphs (Graph Grad CAM) [18] extends CAM on graphs by loosening architecture restrictions and using gradients of hidden layers as projection weights. In this work, we first integrate the localization ability of Graph CAM with the awareness of adversarial attacks on the graph classification tasks. We will undoubtedly increase the scope of research on Graph CAM.

3 PRELIMINARIES

3.1 Notations

Given a set of graphs $\mathcal{G} = \{G_i\}_{i=1}^N$, where $|\mathcal{G}| = N$, we consider graph classification on \mathcal{G} . Each graph $G_i = (\mathbf{A}_i, \mathbf{X}_i)$ has n_i nodes, where $\mathbf{A}_i \in \{0, 1\}^{n_i \times n_i}$ is the adjacency matrix and $\mathbf{X}_i \in \mathbb{R}^{n_i \times D}$ is the node feature matrix with dimension

D . Each G_i is assigned with a label $c_i \in \mathcal{C} = \{1, 2, \dots, C\}$, where C is the total number of classes.

3.2 Graph Classification

Graph classification aims to predict the labels of unlabeled graphs. With paired graphs and labels $\{G_i, c_i\}_{i=\{1, \dots, N\}}$, its goal is to learn a mapping function $f: \mathcal{G} \rightarrow \mathcal{C}$. We simplify graph classification model architecture and consider only one fully connected layer. Given a graph $G_i = (\mathbf{A}_i, \mathbf{X}_i)$ with n_i nodes, a standard procedure for graph classification with direct pooling can be formulated as:

$$\mathbf{h}_i^{(0)} = \mathbf{X}_i, \quad \mathbf{h}_i^{(l)} = f_{conv}(\mathbf{h}_i^{(l-1)}; \Theta^l), \quad l = 1, 2, \dots, L \quad (1)$$

$$\mathbf{h}_i = \text{pooling}(\mathbf{h}_i^{(L)}), \quad \mathbf{z}_i = \mathbf{W}\mathbf{h}_i + \mathbf{b}, \quad (2)$$

where $\mathbf{h}_i^{(l)} \in \mathbb{R}^{n_i \times D_l}$ denotes the hidden node embedding in the l -th graph convolution f_{conv} , and Θ^l is the corresponding parameter matrix. $\mathbf{h}_i \in \mathbb{R}^{D_L}$ is the graph embedding of G_i after pooling of final node embedding $\mathbf{h}_i^{(L)} \in \mathbb{R}^{n_i \times D_L}$. $\mathbf{W} \in \mathbb{R}^{C \times D_L}$ and $\mathbf{b} \in \mathbb{R}^C$ are parameters in the output fully connected layer, and L is the number of graph convolution.

The objective function for graph classification can be further formulated as:

$$\min_{\Theta} \mathcal{L}_{\Theta}(\mathcal{G}) = \sum_{i=1}^N l_{\Theta}(f_{\Theta}(G_i), c_i),$$

where $l(\cdot, \cdot)$ is a loss function such as the cross-entropy.

3.3 Adversarial Attacks towards GNNs

The problem of adversarial attacks on graph classification is to misclassify graph labels, which is formulated as follows:

Problem 1. Given paired data of graphs and their labels $\{G_i, c_i\}_{i=1}^N$, the goal of an attacker is to minimize the attack objective function \mathcal{L}_{atk} :

$$\operatorname{argmin}_{\mathcal{G}'} \mathcal{L}_{atk}(\mathcal{G}') = \sum_{i=1}^N l_{atk}(f_{\Theta}(G'_i), c_i),$$

where l_{atk} is the attack loss function, and G'_i denotes the perturbed version of G_i .

We could define $l_{atk} = -l$ where l is set as the cross-entropy loss for graph classification. We can also define l_{atk} as the other attack loss like the CW-loss [20].

In real-world, the attacker usually only unnoticeably attacks within perturbation budget Δ for each graph G_i . Thus, the domain of modified graphs is constrained as :

$$\| \mathbf{A}'_i - \mathbf{A}_i \|_0 + \| \mathbf{X}'_i - \mathbf{X}_i \|_0 \leq \Delta,$$

where \mathbf{A}'_i and \mathbf{X}'_i are the perturbed adjacency matrix and node feature matrix for graph G'_i . In the following sections, we omit the subscript i for graph G_i for simplicity.

Adversarial attacks have various taxonomies from the perspectives of perturbation type (feature attack and structure attack), attacker's knowledge (white-box attack and black-box attack), and the stage where attacks happen (evasion attack and poisoning attack). A desired general framework should be able to deliberate most situations mentioned above, which is also the aim of this work.

4 METHODOLOGY: A HIERARCHICAL FRAMEWORK

In order to quantify the contribution of nodes at the local level to graph classification tasks at the global level and reversely conduct effective adversarial attacks at the local level to destroy the performance from the global level, we propose to decompose the whole attack precede into two steps hierarchically: 1) *node importance estimation*, and 2) *adversarial example generation*. In this way, we are able to first transfer the focus from classification on graphs to the contribution of each node and design perturbations locally afterward.

4.1 Node Importance Estimation

After finishing model training, we determine the contribution of nodes from local level to graph classification in a way inspired by Graph CAM and its variant [18].

Graph CAM. As a useful method that provides explainability for graph classification, Graph CAM has been well studied. Since the weight matrix of the output fully connected layer can represent the importance of the features of each dimension for graph classification, Graph CAM builds a heat-map matrix by projecting back the weight matrix to the node representation in the final graph convolution layer to indicate the importance of each node for graph classification. This heat-map matrix is calculated as:

$$\mathbf{L}_{CAM} = \text{ReLU}(\mathbf{h}^{(L)} \mathbf{W}^T), \quad (3)$$

where $\mathbf{W} \in \mathbb{R}^{C \times D_L}$ is the same weight matrix as in Eq. (2), and $\mathbf{h}^{(L)} \in \mathbb{R}^{n \times D_L}$ denotes node representation in the final graph convolution layer for one graph as shown in Eq. (1). The k -th element in c -th row of \mathbf{W} indicates the importance of feature k for predicting label c .

A variant of Graph CAM, Graph Grad CAM, uses gradients with respect to each hidden convolutional layer and each class. Then, the calculation of gradients $\alpha^l \in \mathbb{R}^{D^l \times C}$ replaces weights \mathbf{W}^T in CAM to construct the heat-map

matrix for each layer. At last, by taking the average over heat-map matrix of all graph convolution layers, the heat-map matrix is calculated as:

$$\alpha^l = \frac{1}{n} \sum_v \frac{\partial z^T}{\partial \mathbf{h}_v^{(l)}}, \quad \mathbf{L}_{Grad-CAM} = \frac{1}{L} \sum_l \text{ReLU}(\mathbf{h}^{(l)} \alpha^l),$$

where $z \in \mathbb{R}^C$ is the prediction logits, $\mathbf{h}_v^{(l)} \in \mathbb{R}^{D^l}$ is the hidden embedding for node v in the l -th graph convolution layer. The i -th entry in c -th column of \mathbf{L}_{CAM} indicates the relative importance for node i resulting from classifying G_i into class c .

Though having great explainability, directly using Graph CAM still has two limitations. Firstly, the number of fully connected layers is fixed to one due to the restriction on matrix multiplication in Graph CAM. Secondly, the hidden size must be kept the same for all hidden convolutional layers for Graph Grad CAM. As we will show in Experiments, these architecture restrictions do not deteriorate classification performance on clean graphs. Also, they do not hinder the transferability of our proposed attack methods.

Ranked CAM Matrix. We calculate the ranked CAM matrix based on the CAM heat-map matrix. The whole process is summarized in Algorithm 1. After getting the CAM heat-map matrix, We firstly rank each column in a descending order and get the corresponding nodes ranking matrix $\mathbf{U}_{CAM}^{orig} \in \mathbb{R}^{n \times C}$ in line 1. This implies the class-specific view of nodes importance ranking. Then, we exploit \mathbf{U}_{CAM}^{orig} to calculate a global-level nodes ranking vector $\mathbf{u}_{global} \in \mathbb{R}^n$ in line 2. Specifically, we go through each row in \mathbf{U}_{CAM}^{orig} and use the highest ranking among all columns for each node until all nodes are included in \mathbf{u}_{global} . Finally, we concatenate these two ranking sources of nodes to get the final ranked CAM matrix $\mathbf{U}_{CAM} \in \mathbb{R}^{n \times (C+1)}$.

Algorithm 1: Generating ranked CAM matrix.

Input: Heat-map matrix \mathbf{L}_{CAM} .

Output: Ranked CAM matrix \mathbf{U}_{CAM} .

- 1 $\mathbf{U}_{CAM}^{orig} \leftarrow \text{column_rank}(\mathbf{L}_{CAM});$
 - 2 $\mathbf{u}_{global} \leftarrow \text{global_rank}(\mathbf{L}_{CAM});$
 - 3 $\mathbf{U}_{CAM} \leftarrow \text{concatenate}([\mathbf{U}_{CAM}^{orig}, \mathbf{u}_{global}]);$
 - 4 Return $\mathbf{U}_{CAM};$
-

Because CAM heat-map matrix can precisely demonstrate the importance of each node for graph classification tasks, after ranking operation on CAM heat-map, each column in \mathbf{U}_{CAM} indicates one type of view for nodes importance ranking. We could identify the most influential nodes for the whole graph classification process through different views of the ranked CAM matrix and generate adversarial examples accordingly. Since the adversarial attack depends on Graph CAM, we name our hierarchical framework as CAM based Attack and its variant *CAMA-Grad* when using Graph Grad CAM.

4.2 Adversarial Example Generation

With access to the ranked CAM matrix \mathbf{U}_{CAM} , we call each column of \mathbf{U}_{CAM} as the ranked CAM vector, denoted as $\mathbf{U}^c, c = 1, \dots, C + 1$. How do we generate adversarial examples with a series of ranked CAM vectors? Here,

we heuristically propose two attack algorithms towards *CAMA* (for feature attack and structure attack) and *CAMA-subgraph* (for structure attack only). For *CAMA*, in the overall adversarial perturbation, we repeat using our algorithms for each column of ranked CAM matrix U^c until a successful attack. For *CAMA-subgraph*, we only need the column of the predicted label in the ranked CAM matrix to select the candidate perturbations. Both two algorithms have their grad version *CAMA-Grad* and *CAMA-subgraph-Grad*. The difference between algorithms and their grad version lies only in calculating CAM heat-map matrix.

4.2.1 Feature Attack

For feature perturbations, we set both global-level and local-level perturbation budgets. In global-level budgets, we assume only a small number of nodes of one particular graph is available. These nodes are called target nodes. In local-level budgets, we constrain the number of features to be adjusted.

Given the limitation of modified node amount r , target nodes are selected by the first r nodes in ranked CAM vector U^c . A small constant noise ϵ is added to each feature of target nodes for perturbation, while ϵ relies on the attacker’s knowledge of node features. Specifically, given the information of the training process, the number of adjusted features K and adjusted magnitude λ , noise ϵ_j added for the j -th feature could be calculated following [21] as:

$$\epsilon_j = \begin{cases} \lambda \cdot \text{sign} \left(\sum_{i=1}^n \frac{\partial l(f_\theta(G), c)}{\partial X_{ij}} \right), \\ \text{if } j \in \text{argtop-K} \left(\left[\left| \sum_{i=1}^n \frac{\partial l(f_\theta(G), c)}{\partial X_{il}} \right| \right]_{l=1,2,\dots,D} \right) \\ 0, \text{ otherwise.} \end{cases}$$

We replace Carlili-Wagner loss in [21] with cross-entropy loss. The overall number of perturbations is $rK \leq \Delta$. We summarize the process of *CAMA* for generating feature perturbations in Algorithm 2.

Algorithm 2: *CAMA* for feature perturbations.

Input: Graph $G = (\mathbf{A}, \mathbf{X})$ with n nodes; number of nodes limit r ; ranked nodes vector U^c ; feature noise ϵ_j , where $j = 1, 2, \dots, D$.
Output: Modified feature matrix \mathbf{X}' .
1 Initialize modified feature matrix $\mathbf{X}' \leftarrow \mathbf{X}$;
 $C_{nodes} \leftarrow U^c[1:r]$;
2 **for** u in C_{nodes} **do**
3 | $\mathbf{X}'_j[u] \leftarrow \mathbf{X}_j[u] + \epsilon_j$, $j = 1, 2, \dots, D$
4 **return** \mathbf{X}' ;

4.2.2 Structure Attack

Structure attack is more comprehensive compared with feature attack, considering the complexity of connectivity in graphs. To this end, we specially design two structure attack algorithms: *CAMA* and *CAMA-subgraph*, with the help of the ranked CAM matrix. *CAMA* is an efficient algorithm that performs attacks via simply flipping edges among top-ranked vital nodes in the ranked CAM matrix. *CAMA-subgraph* then takes a step further to attack through learning a subgraph mask to select edges for perturbation.

***CAMA*: structure attack by flipping edges among most important nodes.** To generate structure perturbations, we

assume edges among nodes of higher activation importance are more influential in graph classification tasks and intuitively flip edges among them. With the known ranked nodes influence on graph classification, we could flip edges among nodes that have higher ranking. Furthermore, we exploit nodes similarity to enhance attack ability aside from the information from graph structure. The similarity score is calculated as follows.

Given a learned embedding of node h^{emb} , similarity S between nodes u and v is calculated with cosine distance:

$$S[u, v] = S[v, u] = \cos(h_u^{emb}, h_v^{emb}).$$

We constrain the operation of adding/deleting edges within the similarity constraint. Under the graph homophily assumption and with the calculated similarity matrix S , we choose to add edges between low similarity node pairs and delete edges between high similarity node pairs:

$$\begin{cases} \mathbf{A}'[u, v] - \mathbf{A}[u, v] = 1, \mathbf{A}[u, v] = 0 \text{ and } S[u, v] \leq s_1; \\ \mathbf{A}'[u, v] - \mathbf{A}[u, v] = -1, \mathbf{A}[u, v] = 1 \text{ and } S[u, v] \geq s_2. \end{cases}$$

Our attacking strategy is in a heuristic way by increasing ranking number each time, iteratively finding candidate pairs of nodes and flipping edges between new target nodes and old ones within perturbation budget and similarity restriction. In each iteration, we increase ranking number i by one, add a new node u_i , which ranked i -th in vector U^c , into target nodes set C_{nodes} . In the end, we flip edges between new target node and old ones within Δ . The overall procedure for structure perturbations is summarized in Algorithm 3.

Algorithm 3: *CAMA* for structure perturbations.

Input: Graph $G = (\mathbf{A}, \mathbf{X})$ with n nodes; modification budget Δ ; Similarity matrix S ; similarity restriction parameter s_1, s_2 ; ranked nodes vector U^c .
Output: Modified adjacency matrix \mathbf{A}' .
1 Initialize remaining perturbation number $n_{perturbs} \leftarrow \Delta$, modified adjacency matrix $\mathbf{A}' \leftarrow \mathbf{A}$, target nodes set $C_{nodes} = U^c[0]$, and current rank index $i = 1$.
2 **while** ($i \leq n$) and ($n_{perturbs} > 0$) **do**
3 | $u_i \leftarrow U^c[i]$;
4 | **for** v in C_{nodes} **do**
5 | | **if** similarity_constraint((u_i, v) ; S, s_1, s_2) **then**
6 | | | $\mathbf{A}'[u_i, v] \leftarrow 1 - \mathbf{A}[u_i, v]$;
7 | | | $n_{perturbs} \leftarrow n_{perturbs} - 1$;
8 | | | **if** $n_{perturbs} == 0$ **then**
9 | | | | **break**;
10 | $C_{nodes} \leftarrow [C_{nodes}, u_i]$;
11 | $i \leftarrow i + 1$;
12 **Return** \mathbf{A}' ;

***CAMA-subgraph*: structure attack with subgraph mask training.** In order to further exploit the local information from a subgraph perspective, we propose an end-to-end adversarial structure attack model with a subgraph mask.

For each graph G , we obtain a subgraph G_{sub} by keeping $p\%$ top ranked nodes $\mathcal{V}_{sub}, |\mathcal{V}_{sub}| = \lfloor p\%|\mathcal{V}| \rfloor$ in

the nodes rank vector with view of predicted label c (the c -th column U^c in the ranked CAM matrix). Then, we limit potential edge perturbations $M = \mathcal{V}_{sub} \times \mathcal{V}_{sub}$ within the subgraph. With the edge perturbation candidates as subgraph $\{m_{uv} | u, v \in \mathcal{V}_{sub}, \sum_{uv} m_{uv} \leq \Delta\}$, the adversarial examples are calculated as follows:

$$c_{uv} = 1 - 2 * a_{uv} \quad (4)$$

$$a'_{uv} = \begin{cases} a_{uv} + c_{uv} * \sigma(m_{uv}), & u \in \mathcal{V}_{sub}, v \in \mathcal{V}_{sub} \\ a_{uv}, & \text{others,} \end{cases} \quad (5)$$

where $\sigma(\cdot)$ is the sigmoid function to map mask values into zero and one. The larger value of m_{uv} , the more attack importance to perturb edge a_{uv} .

Given a trained victim model f_{Θ} , we minimize the attack loss l_{atk} for each graph with the victim model's parameters unchanged to learn the subgraph mask m_{uv} :

$$\min l_{atk} = l_{cw} + \lambda_{ent} * l_{ent} + \lambda_{size} * l_{size}, \quad (6)$$

where l_{cw} denotes for CW-loss, l_{ent} represents the mean entropy of each element m_{uv} and l_{size} is the penalization term for total mask size. l_{cw} aims to achieve a successful attack [20] and l_{ent} encourages the masking value of $\sigma(m_{uv})$ to be binary [39]. l_{size} restricts the mask's total size to be close to the number of perturbations. For hyper-parameters λ_{ent} and λ_{size} , they balance the influence of l_{cw} , l_{ent} and l_{size} in the total loss function.

Specifically, given the ground truth label c_{yt} of graph, the detailed designs of l_{cw} , l_{ent} and l_{size} are:

$$l_{cw} = \max(z_{c_{yt}} - \max_{c' \neq c_{yt}} z_{c'}, 0), \quad (7)$$

$$l_{ent} = -\frac{1}{|M|} \sum_{u,v \in \mathcal{V}_{sub}} (\sigma(m_{uv}) \log \sigma(m_{uv}) + (1 - \sigma(m_{uv})) \log(1 - \sigma(m_{uv}))), \quad (8)$$

$$l_{size} = \max(|\sum_{u,v \in \mathcal{V}_{sub}} \sigma(m_{uv}) - \Delta| - \eta, 0), \quad (9)$$

where the hyper-parameter η is the confidence size controlling how many entries in m_{uv} could be free of penalization.

Algorithm 4 shows the whole attacking process of structure attack with subgraph mask training, and we denote it as *CAMA-subgraph*. First, we select top-ranked nodes in U^c to formulate a subgraph and limit the edge perturbation within the subgraph in line 1. Secondly, for each training epoch, we minimize the attack loss l_{atk} to train the subgraph mask M as shown in line 4. Then, we select the top-ranked mask M_{Δ} within the perturbation budget Δ in line 6. In lines 7-9, we flip edges for nodes pair selected in M_{Δ} to generate the adversarial example. Finally, we test the attack performance of generated adversarial examples in lines 11-12.

4.3 Complexity Analysis

We analyze the complexity of the proposed framework by using *CAMA* as an example. Given a graph with n nodes as target, the main complexity lies in the preparation of inputs:

Algorithm 4: *CAMA-subgraph* for structure attack.

Input: Graph $G = (A, X)$ with n nodes; the ground truth label c_{gt} of graph G ; ranked nodes vector of the predicted label U^c ; subgraph proportion $p\%$; victim model f_{Θ} ; total training epoch number T ; the perturbation budget Δ ;

Output: Modified Adjacency matrix A' .

```

1 Initialize perturbation candidate subgraph
   $\mathcal{V}_{sub} = \{u | u \in U^c[: n_{sub}]\}$ , where  $n_{sub} = \lfloor p\%|\mathcal{V}| \rfloor$ .
2 for  $t$  in  $1, 2, \dots, T$  do
3   // Train subgraph mask
4    $\min_M l_{atk} = l_{cw} + \lambda_{ent} * l_{ent} + \lambda_{size} * l_{size}$ ;
5   // Generate the adversarial example
6   select top  $\Delta$  perturbations  $M_{\Delta} \subset M$ ;
7   for  $(u, v) \in \{(u, v) | m_{uv} \in M_{\Delta}\}$  do
8      $a'_{uv} \leftarrow 1 - a_{uv}$ ;
9    $G' \leftarrow (A', X)$ ;
10  // Test the adversarial example
11  if  $\arg \max_c f_{\Theta}(G') \neq c_{gt}$  then
12    break;
13 return  $A'$ ;
```

- The original nodes ranking matrix U_{CAM}^{orig} (Algorithm 1): The complexity of line 1 is $\mathcal{O}(Cn \log(n)) = \mathcal{O}(n \log(n))$, since the number of classes is always much less than that of nodes. Then the complexity from line 2 to 6 is $\mathcal{O}(Cn)$. Thus the total complexity of Algorithm 1 is $\mathcal{O}(n \log(n) + Cn)$;
- Feature noise ϵ_j , where $j = 1, 2, \dots, D_L$: The complexity of getting all ϵ is $\mathcal{O}(nD_L + nK) = \mathcal{O}(nD_L)$, since K is selected from D_L ;
- Similarity matrix S : The complexity of having similarity matrix is $\mathcal{O}(n^2 D_L)$.

Then we analyze the complexity of Algorithm 2 and 3 accordingly, note that all constraints have no effects on the complexity since they can be checked in constant time:

Feature attack (Algorithm 2). The complexity from line 3 to line 5 is $\mathcal{O}(r)$. Thus, the total complexity of Algorithm 2 is combining it with U^c and all ϵ , which is $\mathcal{O}(n \times \max(D_L, \log(n)))$.

Structure attack (Algorithm 3). The complexity from line 2 to line 11 is $\mathcal{O}(\min(n^2, \Delta))$. Thus, combining with the complexity of similarity matrix S , the total complexity of Algorithm 3 is $\mathcal{O}(\min(n^2 D_L, \Delta)) = \mathcal{O}(\Delta)$, since the modification budget Δ is controlled to restrict the access from attackers and strictly smaller than n^2 .

Through our analysis of the complexity above, we can find that *CAMA* enjoys computational efficiency, especially in comparison with the complexity of target GNNs.

5 EXPERIMENTS

5.1 Experimental Setups

Datasets. We evaluate our attack strategies on four chemical graph classification benchmarks: MUTAG, PROTEINS, NCI1, COX2 [40], and two social network datasets: IMDB-BINARY, IMDB-MULTI. Among chemical graphs, node features consist of node attributes and node labels: in PROTEINS and COX2, we use both node labels and attributes, while in the

TABLE 1: Dataset statistics.

Models	# of Graphs	# of Classes	Avg. # of Nodes	Avg. # of Edges
MUTAG	188	2	17.93	19.79
PROTEINS	1113	2	39.06	72.82
NCI1	4110	2	29.87	32.3
COX2	467	2	41.22	43.45
IMDB-BINARY	1000	2	19.77	96.53
IMDB-MULTI	1500	3	13.00	65.94

TABLE 2: Summary of the change in classification accuracy (in %) compared to the clean graph under **white-box attack** for **chimecal datasets**. Lower is better. Best performances are shown in **bold** markers.

Dataset	MUTAG				PROTEINS				NCI1				COX2			
	GCN	GIN-0	IGNN	g-U-Nets	GCN	GIN-0	IGNN	g-U-Nets	GCN	GIN-0	IGNN	g-U-Nets	GCN	GIN-0	IGNN	g-U-Nets
Clean	83.04	89.85	81.46	88.89	78.17	77.81	77.99	77.54	78.98	77.59	75.06	72.24	88.87	83.51	83.51	83.08
	<i>Feature attack</i>															
<i>Random</i>	-5.35	-5.29	-7.43	-7.02	-1.26	-0.63	-4.04	-0.90	-16.06	-19.03	-33.92	-55.57	-17.32	-3.42	-7.05	-11.54
<i>Degree</i>	-4.82	-7.40	-7.43	-8.66	-1.61	-0.81	-4.58	-0.99	-17.27	-23.63	-37.40	-59.37	-22.67	-4.28	-8.54	-13.90
<i>GradArgmax-fea</i>	-5.88	-7.43	-7.43	-5.91	-1.35	-0.90	-4.40	-0.81	-18.73	-22.48	-39.76	-55.26	-40.85	-7.72	-10.73	-12.41
<i>ReWatt-fea</i>	-2.13	-3.16	-2.63	-2.75	-0.36	-0.72	-2.15	-0.45	-11.29	-14.60	-19.71	-31.80	-15.38	-3.63	-6.62	-4.48
<i>CAMA</i>	-10.64	-9.53	-10.12	-11.78	-2.24	-1.44	-6.56	-2.25	-33.58	-36.08	-56.74	-69.61	-52.68	-9.69	-27.83	-27.64
<i>CAMA-Grad</i>	-11.70	-9.53	-10.12	-11.73	-2.60	-1.53	-6.29	-2.25	-31.70	-35.57	-56.76	-69.90	-52.23	-15.47	-22.89	-24.40
	<i>Structure attack</i>															
<i>Random</i>	-4.82	-16.43	-5.26	-2.13	-0.99	-4.13	-1.53	-0.54	-9.49	-10.97	-6.37	-4.31	-6.43	-3.84	-2.14	-4.93
<i>Degree</i>	8.48	-16.43	-7.92	-3.27	-0.72	-6.91	-1.53	-0.09	-8.08	-15.13	-5.79	-4.31	-6.87	-9.83	-4.07	-5.56
<i>GradArgmax</i>	-7.98	-43.33	-7.37	-2.13	-1.88	-7.63	-2.96	-1.08	-10.90	-12.31	-10.85	-7.45	-17.17	-16.24	-13.08	-11.99
<i>ReWatt</i>	-4.24	-13.77	-4.74	-8.60	-0.72	-1.89	-0.72	-0.54	-7.64	-5.89	-4.72	-2.90	-2.58	-7.94	-1.29	-1.28
<i>CAMA</i>	-11.08	-47.08	-11.64	-9.18	-3.23	-9.44	-2.88	-1.35	-20.68	-22.43	-15.74	-9.88	-22.47	-18.89	-13.93	-12.64
<i>CAMA-Grad</i>	-11.64	-50.20	-12.72	-5.85	-2.78	-9.16	-3.24	-1.08	-23.50	-22.29	-16.69	-8.76	-24.86	-18.85	-13.28	-15.81
<i>CAMA-subgraph</i>	-12.25	-59.09	-7.92	4.24	-7.39	-37.31	-7.57	-6.67	-37.15	-44.74	-41.77	-20.41	-28.84	-56.25	-30.53	-14.34
<i>CAMA-subgraph-Grad</i>	-12.75	-56.99	-11.14	1.00	-6.94	-37.40	-7.93	-6.94	-38.20	-44.38	-40.34	-19.29	-27.77	-56.46	-24.98	-10.24

TABLE 3: Summary of the change in classification accuracy (in %) compared to the clean graph under **white-box attack** for **social networks**. Lower is better. Best performances are shown in **bold** markers.

Dataset	IMDB-BINARY			IMDB-MULTI		
	GCN	GIN	g-U-Nets	GCN	GIN	g-U-Nets
Clean	73.67	74.22	73.89	50.00	50.59	48.30
<i>Random</i>	-0.78	-7.55	-0.78	-0.96	-9.48	-0.45
<i>Degree</i>	-1.67	-18.00	-2.78	-1.63	-14.37	-2.37
<i>GradArgmax</i>	-4.34	-19.22	-3.33	-2.82	-14.52	-1.11
<i>ReWatt</i>	-6.07	-3.22	-6.99	-6.53	-2.79	-3.03
<i>PGD</i>	-2.57	-22.82	-1.79	-2.00	-29.12	-0.57
<i>CAMA</i>	-2.11	-15.22	-2.33	-3.11	-11.48	-1.19
<i>CAMA-Grad</i>	-2.78	-15.55	-1.56	-3.26	-13.33	-1.04
<i>CAMA-subgraph</i>	-7.47	-21.72	-7.99	-7.00	-30.26	-3.63
<i>CAMA-subgraph-Grad</i>	-7.07	-24.22	-7.89	-7.27	-29.79	-3.50

TABLE 4: Summary of the change in classification accuracy (in %) compared to the clean graph under **black-box attack**. Lower is better.

Dataset	MUTAG			PROTEINS			NCI1			COX2		
	GIN-0	IGNN	g-U-Nets	GIN-0	IGNN	g-U-Nets	GIN-0	IGNN	g-U-Nets	GIN-0	IGNN	g-U-Nets
Clean	89.85	81.46	88.89	77.81	77.99	77.54	77.59	75.06	72.24	83.51	83.51	83.08
	<i>Feature attack</i>											
<i>Random</i>	-2.13	-4.24	-4.85	-0.54	-3.59	-0.45	-6.59	-9.32	-13.14	-2.56	-7.26	-9.19
<i>Degree</i>	-2.66	-4.24	-6.52	-0.63	-4.13	-0.54	-9.46	-10.19	-14.89	-3.85	-7.69	-10.69
<i>GradArgmax-fea</i>	-3.19	-3.68	-4.30	-0.45	-3.32	-0.45	-6.72	-13.41	-13.67	-7.50	-11.75	-9.19
<i>ReWatt-fea</i>	-3.16	-2.63	-2.75	-0.72	-2.15	-0.45	-14.60	-19.71	-31.80	-3.63	-6.62	-4.48
<i>CAMA</i>	-4.24	-6.93	-5.38	-0.90	-5.57	-1.26	-17.13	-23.72	-24.28	-12.88	-22.04	-22.26
<i>CAMA-Grad</i>	-3.71	-8.01	-4.27	-0.99	-5.84	-1.17	-15.23	-22.65	-24.06	-12.44	-19.03	-20.35
	<i>Structure attack</i>											
<i>Random</i>	-16.43	-5.26	-2.13	-4.13	-1.53	-0.54	-10.97	-6.37	-4.31	-3.84	-2.14	-4.93
<i>Degree</i>	-16.43	-7.92	-3.27	-6.91	-1.53	-0.09	-15.13	-5.79	-4.31	-9.83	-4.07	-5.56
<i>GradArgmax</i>	-12.75	-9.53	-2.72	-5.48	-1.17	-0.90	-8.88	-6.67	-3.75	-9.82	-4.48	-5.12
<i>ReWatt</i>	-13.77	-4.74	-8.60	-1.89	-0.72	-0.54	-5.89	-4.72	-2.90	-7.94	-1.29	-1.28
<i>CAMA</i>	-25.44	-10.58	-8.16	-10.42	-2.43	-1.71	-19.03	-11.41	-8.30	-13.91	-10.48	-8.34
<i>CAMA-Grad</i>	-27.54	-11.08	-9.21	-11.68	-2.87	-1.62	-19.63	-16.03	-9.51	-16.69	-9.63	-9.84
<i>CAMA-subgraph</i>	-54.42	-13.21	-11.23	-24.98	-6.02	-5.39	-37.08	-20.41	-16.30	-53.52	-21.00	-15.00
<i>CAMA-subgraph-Grad</i>	-53.39	-13.77	-11.76	-24.16	-5.93	-5.39	-37.86	-21.78	-17.45	-53.31	-16.27	-14.58

others, we only use one-hot node labels as node features. For social networks, node features are initialized with the node degree. The datasets statistics can be found in Table 1.

Graph Classifiers. We use four state-of-the-art GNNs for graph classification: GCN, GIN, IGNN and g-U-Nets. For all configurations, only one full connected layer is adopted and no dropout layer used after graph pooling. A same global sum-pooling readout function is applied for all models. For GCN, we use 5 GCN convolutional layers. For GIN, we set $\epsilon = 0$ (also called GIN-0) and use 5 GIN convolution layers. For IGNN, we use 3 IGNN convolution layers and tune hyper-parameter $\kappa \in \{0.7, 0.98\}$. g-U-Nets have a different architecture due to their hierarchical nature. Here, we use node representation of the last layer before readout function to calculate the CAM heat-map matrix. We apply four gPool layers with respectively 90%, 70%, 60%, and 50% nodes proportions and ignore max-pooling layer in its readout function since global max-pooling is poorer at localization compared to GAP [37]. We implement these GNNs with Pytorch Geometric (PyG)¹.

Baselines. We compare our methods with five baselines as follows. Every baseline we compared either released source code, or made it available upon request.

- *Random* [13]: *Random* randomly selects nodes to perturb and edges to insert/delete.
- *Degree* [41]: *Degree* chooses nodes with top degrees and insert/delete edges among them.
- *GradArgmax* [13]: *GradArgmax* greedily selects perturbation edges by gradients of each pair of nodes, which works only for structure attack. We choose *GradArgmax* as a representative of the white-box attack baseline.
- *PGD* [12]: *PGD* performs the project gradient descent topology attack and is an effective white-box attack algorithm.
- *ReWatt* [32]: *ReWatt* conducts rewiring operations to perform structure attacks and uses reinforcement learning to find the optimal rewiring operations. We select *ReWatt* as the representative of the state-of-the-art black-box optimization baseline.

In order to enrich the feature attack baseline, we generate two variants, *GradArgmax-fea* and *ReWatt-fea*, to perform feature attacks. In particular, we select end points of the perturbed edges by *GradArgmax* as victim nodes, and then add noises to them. For *ReWatt-fea*, we change the action space to feature manipulation of selected nodes by rewiring. A validate action contains perturbations on three nodes, that is, one center node, its one-hop neighbor and two-hop neighbor. Because an edge contains two end nodes and a rewire operation is related to three nodes, we ensure that the number of nodes manipulated by *GradArgmax* and *ReWatt* is more than or equal to that of *CAMA* to make a fair comparison.

Perturbation restrictions and hyper-parameters. For feature attack, we set feature adjusted magnitude $\lambda = 0.1$. We select 10% of nodes in one graph to perturb, and 10% of features are modified for each dataset. For structure attack, we set the perturbation budget $\Delta = \lceil 10\%|E_i| \rceil$ for each graph G_i , where $|E_i|$ denotes the number of edges in graph G_i . For *ReWatt*, the number of rewiring operations are set to $\lceil 0.5\Delta \rceil$ with at least one rewiring, which is kept the same

setting as [32]. Besides, in the similarity restriction, we use the first hidden layer to calculate nodes similarity $h^{emb} = h^{(1)}$, fix $s_2 = 0.95$ and tune $s_1 \in \{0.95, 0.9, 1\}$. For *CAMA-subgraph*, we set total training epochs as 200, the subgraph graph proportion $p\% = 50\%$, $\lambda_{ent} = 1$, $\lambda_{size} = 10$ and the confidence size $\eta = 3$.

We conduct untargeted attack and evaluate on test graphs. Specifically, we perform 10-fold cross-validation in each classification process and report the average validation accuracy within the cross validation. This configuration follows [23] on graph classification, resulting from the unstable training of small-sized datasets such as MUTAG.

5.2 Adversarial Attack on Graph Classification

We first compare *CAMA* and *CAMA-subgraph* to multiple baselines under the white-box attack. We train on clean graphs for each graph classifier, generate perturbed graphs on validation sets, and calculate prediction accuracy using the trained graph classifiers. Full results under white-box setting for chemical datasets are provided in Table 2, for social networks are demonstrated in Table 3.

In feature attack, our proposed methods performs better by a high margin on all datasets and all graph classification models, which implies our methods can select the most influential nodes for graph classification tasks. In structure attack, *CAMA* and *CAMA-subgraph* outperform the other baselines in all situations. Meanwhile, the subgraph mask training algorithm (*CAMA-subgraph*) outperforms the simple heuristic flip edge method (*CAMA*) by a large margin. Actually, the choice of *CAMA* and *CAMA-subgraph* is to balance the attack efficiency and effectiveness. These results demonstrate the high attack effectiveness of *CAMA*. More interestingly, the grad version *CAMA-Grad* achieves excellent performance close to *CAMA* but does not guarantee better performance.

We also observe that the attack results vary from different datasets and graph classifiers. The accuracy decreases the least on PROTEINS dataset when suffering attacks. Interestingly, graph classifiers tend to behave differently when they are attacked by structure and feature perturbations. For example, IGNN is more robust facing structural perturbations while more vulnerable under feature attack.

5.3 Transferability of attack

In real-world applications, model parameters usually are not available. Thus, to evaluate *CAMA* under a more realistic and general situation and further explore the transferability of various attacking methods, we validate our attack strategies under the black-box attack setting for four datasets. Specifically, we use GCN as the surrogate model, generate adversarial examples through targeting GCN, then evaluate the other GNNs on the perturbed graphs. The detailed results are provided in Table 4.

First, we could see our approaches surpass the other baselines in most situations. The perturbations generated by *CAMA* and *CAMA-subgraph* consistently demonstrate strong transferability on four graph classification datasets under black-box attack setting. For *CAMA-subgraph*, we could also see a significant performance improvement of *CAMA-subgraph* over *CAMA*. The calculation of the ranked CAM

1. https://github.com/rusty1s/pytorch_geometric

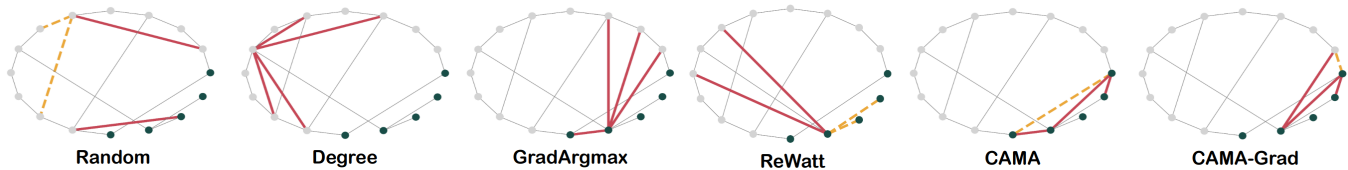


Fig. 3: An example of structure attack on MUTAG dataset with edge attack proportion=20%. Green nodes are selected by CAMA, indicating their strong influences on graph classification. Added edges are shown in red lines and deleted edges are shown in orange dashed lines.

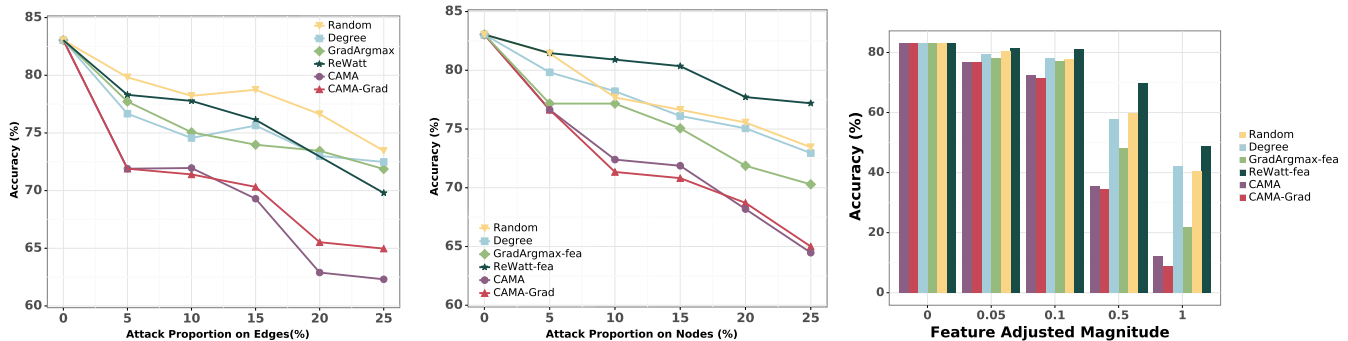


Fig. 4: Attack results with different perturbation hyper-parameters. All experiments are conducted on MUTAG dataset using GCN. Lower accuracy is better. Left: attack results with increasing perturbation proportion of edges. Middle: attack results with increasing perturbation proportion of nodes. Right: attack results with increasing adjusted magnitude values.

matrix and the selected subgraph is important. As a result, the attack performance of a black-box attack may exceed a white-box attack due to an efficient ranked CAM matrix of the GCN surrogate model. Moreover, we could see that the attack performance of *ReWatt* is unstable. It does work with some datasets, like NCI1, while it fails for the other datasets. Second, compared with the white-box attack, our approaches have a more significant advantage over baselines like *GradArgmax*. This indicates that our methods have more vital attack ability when transferring to other GNNs. Besides, the results show that perturbations against a surrogate model with typical architecture could also generalize to the hierarchical graph classifier like g-U-Nets.

5.4 Ablation Studies

Sensitivity analysis for subgraph proportion p in *CAMA-subgraph*. The choice of subgraph proportion in *CAMA-subgraph* is crucial. A larger proportion means more perturbation candidates but also more noise, while a smaller proportion may face perturbation candidates deficiency. An efficient subgraph selection could help the attacker localize the essential subgraph nodes and edges. Figure 5 shows the attack performance of *CAMA-subgraph* with various subgraph proportion on MUTAG. We could see a clear drop tendency when the subgraph proportion gets smaller from 100%, which indicates the effectiveness of locating the subgraph with the ranked CAM vector. For MUTAG, the best proportion is 60% and the accuracy drop 14.36% under this structure attack perturbation setting.

Sensitivity analysis for λ_{size} in *CAMA-subgraph*. Table 5 displays the changes of test accuracy when the hyper-parameters λ_{size} in Eq.(6) are changed in *CAMA-subgraph*. The test accuracy decreases and then increases when λ_{size}

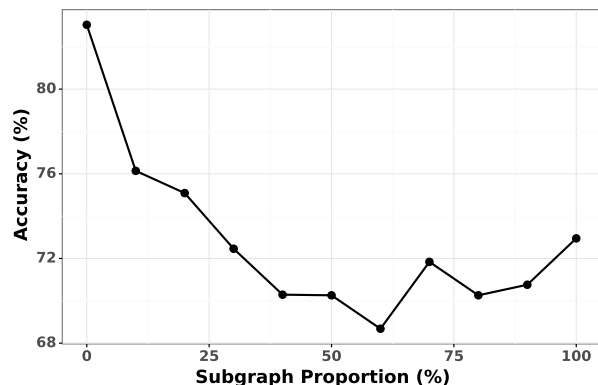


Fig. 5: Line-plot for attack performance under *CAMA-subgraph* for different subgraph proportion. We record 10-fold testing results on MUTAG dataset using GCN as graph classifier. Lower is better.

gets larger from zero. We could notice that λ_{size} does promote a better attack performance compared without it ($\lambda_{size} = 0$). Worth to mention that, λ_{ent} is not that sensitive comparing with λ_{size} .

TABLE 5: Sensitivity analysis for hyper-parameter λ_{size} . Lower is better.

λ_{size}	0	1	5	10	15	20	25
Test Accuracy(%)	73.48	68.16	69.21	70.79	71.35	71.90	72.43

Sensitivity Analysis for Hyper-parameter s_1 and s_2 in *CAMA*. We perform a sensitivity analysis over s_1 and s_2 in Table 6 and set GIN as the victim model on MUTAG

dataset. s_1 controls the edge insertion and s_2 controls the edge deletion. $s_1 = 1, s_2 = 0$ represents no restriction on edge insertion/deletion. We could find that controlling the edge insertion is more helpful for successful attacks contrast to edge deletion.

TABLE 6: Sensitivity analysis for hyper-parameter s_1 and s_2 . Lower is better.

Hyper-parameter	clean	0	0.2	0.4	0.6	0.8	1
s_1 (fix $s_2=0$)	83.04	67.72	67.72	66.64	67.16	66.64	71.40
s_2 (fix $s_1=1$)	83.04	71.40	71.40	71.93	71.93	71.93	72.46

Perturbations budget for white-box attack. We analyze the changes of accuracy with respect to the perturbation budget from Figure 4. Not surprisingly, the prediction accuracy decreases with higher number of perturbations or larger values of adjusted magnitude. In all settings of hyper-parameters, we can observe that *CAMA* and *CAMA-Grad* show remarkable advantages over all the other baselines. Meanwhile, from the figure on the right, we could observe the accuracy drops dramatically when the adjusted magnitude λ gets larger for *CAMA* and *CAMA-Grad*.

5.5 Visualization of selected nodes and adversarial edges

We visualize our selected important nodes from *CAMA* and *CAMA-Grad*, then compare the generated structural perturbations with different baselines in Figure 3. Among all attacking strategies, edges selected by *CAMA* and *CAMA-Grad* are more concentrated on important nodes for graph classification while the other methods are not. For example, for *Degree*, structure attack is generated based on degree. This may result in irrelevant perturbation between nodes and edges. Meanwhile, we can observe that the adversarial edges produced by *GradArgmax* and *ReWatt* are trapped near one single node, which further implies the deficiency of these two methods that extract merely local information.

TABLE 7: Statistics for selected nodes by *CAMA* and *Degree*.

Method	Avg. Degree	Avg. Closeness	Total Variation	No. Edges
<i>Degree</i>	2.8	0.25	12	1
<i>CAMA</i>	2.4	0.22	8	2

Insights of target nodes chosen by *CAMA*. We compare top 5 nodes selected by *CAMA* and *Degree* and report statistics in Table 7. The relatively small average degree and closeness centrality value differentiates *CAMA* from centrality-based methods. Through the total variation and number of edges, we find that nodes chosen by *CAMA* have higher connectivity and smoothness (smaller total variation). Besides, we provide an example of edge perturbations on baselines in Figure 3.

5.6 Computational efficiency analysis

To cooperate with our complexity analysis in Section 4.3, we demonstrate the computational efficiency of *CAMA* and *CAMA-subgraph* in Table 8 by reporting the average running time over 10 times in comparison with all baselines. We can find that *CAMA* can finish within 1.5 second, which is consistent with our complexity analysis and implies that the

scalability of our proposed approaches could not be an issue. The time cost of *CAMA-subgraph* is comparable with *ReWatt*. Both methods need end-to-end training, but *CAMA-subgraph* has better attack performance.

TABLE 8: Running time (s) comparison over all baseline methods on MUTAG using GCN. We report the 10 times average running time within 10-fold cross validation.

Models	<i>Random</i>	<i>Degree</i>	<i>GradArgmax</i>	<i>ReWatt</i>	<i>CAMA</i>	<i>CAMA-Subgraph</i>
Structure	0.3694	0.3820	0.3429	30.0120	0.7888	34.2288
Feature	0.6252	0.6110	0.7538	44.0460	0.6747	-

5.7 Poisoning black-box attack

We also evaluate our methods under poisoning black-box attack. We select GIN as the victim model and retrain it on perturbed graphs generated from the surrogate GCN. Additionally, we compare *CAMA* with a more powerful attacker, project gradient descent topology attack (*PGD*) [12]. *PGD* was originally designed for node classification tasks. We extend its application domain to graph classification. We use cross entropy loss and fix epoch numbers to 10 in our experiment under *PGD* topology attack. Figure 6 shows the final attack results. Coordinating with the results of evasion attack above, the strong transferability of *CAMA* and *CAMA-Grad* still concludes. However, the method using purely gradient information like *GradArgmax* and *PGD* may damage the attacking performance when transferring to other models.

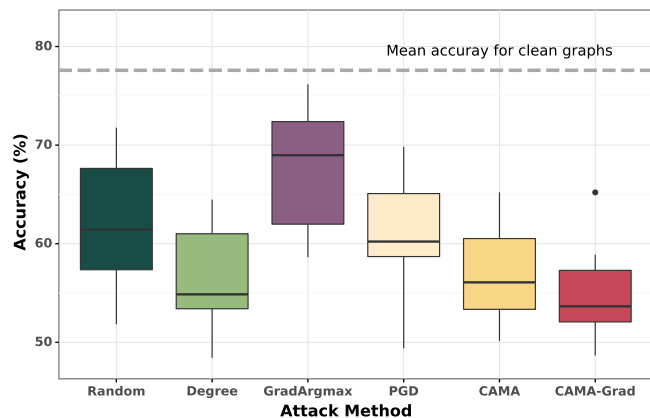


Fig. 6: Box-plot for poisoning structural perturbations under black-box attack. We use GIN as the victim model and record 10-fold testing results on NCI1 dataset. Lower is better.

6 CONCLUSION

In this paper, we establish a general attack framework focusing on graph classification which considers comprehensive attack settings under white-box and black-box attack, and performs both structure attack and feature attack. We hierarchically decompose the novel problem of linking the local-node-level knowledge with global-level graph classification task into two steps. In the first step, we estimate the importance of nodes towards the graph classification by Class Activation Mapping and its variant. Then in the second step, we heuristically design two algorithms to generate adversarial examples for both feature and structure attack with the ranking information of nodes. Experiments show

that the proposed attack strategies significantly outperform existing approaches on various graph classifiers under various settings. Our general framework can also serve as a simple yet novel baseline for future works in the research branch of evaluating the robustness on graph classification tasks.

REFERENCES

- [1] T. N. Kipf and M. Welling, "Semi-supervised classification with graph convolutional networks," *international conference on learning representations*, 2017.
- [2] M. Zhang and Y. Chen, "Link prediction based on graph neural networks," in *Proceedings of the 32nd International Conference on Neural Information Processing Systems*, 2018, pp. 5171–5181.
- [3] Z. Zhang, P. Cui, and W. Zhu, "Deep learning on graphs: A survey," *IEEE Transactions on Knowledge and Data Engineering*, 2020.
- [4] J. Gilmer, S. S. Schoenholz, P. F. Riley, O. Vinyals, and G. E. Dahl, "Neural message passing for quantum chemistry," *international conference on machine learning*, pp. 1263–1272, 2017.
- [5] Z. Zhang, P. Cui, and W. Zhu, "Deep learning on graphs: A survey," *IEEE Transactions on Knowledge and Data Engineering*, 2020.
- [6] F. Monti, F. Frasca, D. Eynard, D. Mannion, and M. M. Bronstein, "Fake news detection on social media using geometric deep learning," *arXiv preprint arXiv:1902.06673*, 2019.
- [7] L. G. Gómez, B. Chiem, and J.-C. Delvenne, "Dynamics based features for graph classification," *arXiv preprint arXiv:1705.10817*, 2017.
- [8] R. Kim, C. H. So, M. Jeong, S. Lee, J. Kim, and J. Kang, "Hats: A hierarchical graph attention network for stock movement prediction," *arXiv preprint arXiv:1908.07999*, 2019.
- [9] T. Magelinski, D. Beskow, and K. M. Carley, "Graph-hist: Graph classification from latent feature histograms with application to bot detection," in *Proceedings of the AAAI Conference on Artificial Intelligence*, vol. 34, 2020, pp. 5134–5141.
- [10] W. Jin, Y. Ma, X. Liu, X. Tang, S. Wang, and J. Tang, "Graph structure learning for robust graph neural networks," in *Proceedings of the 26th ACM SIGKDD International Conference on Knowledge Discovery & Data Mining*, 2020, pp. 66–74.
- [11] S. Bhattacharyya, S. Jha, K. Tharakunnel, and J. C. Westland, "Data mining for credit card fraud: A comparative study," *Decision Support Systems*, vol. 50, no. 3, pp. 602–613, 2011, on quantitative methods for detection of financial fraud.
- [12] K. Xu, H. Chen, S. Liu, P.-Y. Chen, T.-W. Weng, M. Hong, and X. Lin, "Topology attack and defense for graph neural networks: An optimization perspective," in *International Joint Conference on Artificial Intelligence (IJCAI)*, 2019.
- [13] H. Dai, H. Li, T. Tian, X. Huang, L. Wang, J. Zhu, and L. Song, "Adversarial attack on graph structured data," in *International conference on machine learning*. PMLR, 2018, pp. 1115–1124.
- [14] H. Chang, Y. Rong, T. Xu, W. Huang, H. Zhang, P. Cui, W. Zhu, and J. Huang, "A restricted black-box adversarial framework towards attacking graph embedding models," in *Proceedings of the AAAI Conference on Artificial Intelligence*, vol. 34, 2020, pp. 3389–3396.
- [15] H. Wu, C. Wang, Y. Tyshetskiy, A. Docherty, K. Lu, and L. Zhu, "Adversarial examples for graph data: Deep insights into attack and defense," in *Proceedings of the 28th International Joint Conference on Artificial Intelligence*. AAAI Press, 2019, pp. 4816–4823.
- [16] A. Bojchevski and S. Günnemann, "Adversarial attacks on node embeddings via graph poisoning," in *Proceedings of the 36th International Conference on Machine Learning, ICML*, ser. Proceedings of Machine Learning Research. PMLR, 2019.
- [17] A. Bojchevski and S. Günnemann, "Adversarial attacks on node embeddings via graph poisoning," in *Proceedings of the 36th International Conference on Machine Learning, ICML*, ser. Proceedings of Machine Learning Research. PMLR, 2019.
- [18] P. E. Pope, S. Kolouri, M. Rostami, C. E. Martin, and H. Hoffmann, "Explainability methods for graph convolutional neural networks," in *Proceedings of the IEEE/CVF Conference on Computer Vision and Pattern Recognition*, 2019, pp. 10772–10781.
- [19] H. Chang, Y. Rong, T. Xu, W. Huang, S. Sojoudi, J. Huang, and W. Zhu, "Spectral graph attention network with fast eigen-approximation," *arXiv preprint arXiv:2003.07450*, 2020.
- [20] D. Zügner, A. Akbarnejad, and S. Günnemann, "Adversarial attacks on neural networks for graph data," in *Proceedings of the 24th ACM SIGKDD International Conference on Knowledge Discovery & Data Mining*, 2018, pp. 2847–2856.
- [21] J. Ma, S. Ding, and Q. Mei, "Towards more practical adversarial attacks on graph neural networks," *Advances in Neural Information Processing Systems*, vol. 33, 2020.
- [22] C. Guan, Z. Zhang, H. Li, H. Chang, Z. Zhang, Y. Qin, J. Jiang, X. Wang, and W. Zhu, "Autogl: A library for automated graph learning," *arXiv preprint arXiv:2104.04987*, 2021.
- [23] K. Xu, W. Hu, J. Leskovec, and S. Jegelka, "How powerful are graph neural networks," in *ICLR 2019 : 7th International Conference on Learning Representations*, 2019.
- [24] F. Gu, H. Chang, W. Zhu, S. Sojoudi, and L. El Ghaoui, "Implicit graph neural networks," in *Advances in Neural Information Processing Systems*, vol. 33, 2020, pp. 11 984–11 995.
- [25] J. Zhou, G. Cui, S. Hu, Z. Zhang, C. Yang, Z. Liu, L. Wang, C. Li, and M. Sun, "Graph neural networks: A review of methods and applications," *AI Open*, vol. 1, pp. 57–81, 2020.
- [26] Z. Ying, J. You, C. Morris, X. Ren, W. Hamilton, and J. Leskovec, "Hierarchical graph representation learning with differentiable pooling," *neural information processing systems*, pp. 4801–4811, 2018.
- [27] Y. Ma, S. Wang, C. C. Aggarwal, and J. Tang, "Graph convolutional networks with eigenpooling," in *Proceedings of the 25th ACM SIGKDD International Conference on Knowledge Discovery & Data Mining*, 2019, pp. 723–731.
- [28] H. Gao and S. Ji, "Graph u-nets," in *International Conference on Machine Learning*, 2019, pp. 2083–2092.
- [29] W. Jin, Y. Li, H. Xu, Y. Wang, and J. Tang, "Adversarial attacks and defenses on graphs: A review and empirical study," *arXiv preprint arXiv:2003.00653*, 2020.
- [30] D. Zügner, A. Akbarnejad, and S. Günnemann, "Adversarial attacks on neural networks for graph data," in *Proceedings of the 24th ACM SIGKDD International Conference on Knowledge Discovery & Data Mining*, 2018, pp. 2847–2856.
- [31] D. Zügner and S. Günnemann, "Adversarial attacks on graph neural networks via meta learning," in *International Conference on Learning Representations (ICLR)*, 2019.
- [32] Y. Ma, S. Wang, T. Derr, L. Wu, and J. Tang, "Graph adversarial attack via rewiring," in *Proceedings of the 27th ACM SIGKDD Conference on Knowledge Discovery & Data Mining*, ser. KDD '21, 2021, p. 1161–1169.
- [33] X. Wan, H. Kenlay, B. Ru, A. Blaas, M. Osborne, and X. Dong, "Adversarial attacks on graph classifiers via bayesian optimisation," in *Thirty-Fifth Conference on Neural Information Processing Systems*, 2021.
- [34] H. Zhang, B. Wu, X. Yang, C. Zhou, S. Wang, X. Yuan, and S. Pan, "Projective ranking: A transferable evasion attack method on graph neural networks," in *Proceedings of the 30th ACM International Conference on Information & Knowledge Management*, ser. CIKM '21. Association for Computing Machinery, 2021, p. 3617–3621.
- [35] H. Tang, G. Ma, Y. Chen, L. Guo, W. Wang, B. Zeng, and L. Zhan, "Adversarial attack on hierarchical graph pooling neural networks," *arXiv preprint arXiv:2005.11560*, 2020.
- [36] J. Chen, D. Zhang, Z. Ming, and K. Huang, "Graphhacker: A general multi-task graphattack framework," 2021.
- [37] B. Zhou, A. Khosla, A. Lapedriza, A. Oliva, and A. Torralba, "Learning deep features for discriminative localization," in *Proceedings of the IEEE conference on computer vision and pattern recognition*, 2016, pp. 2921–2929.
- [38] H. Yuan, H. Yu, S. Gui, and S. Ji, "Explainability in graph neural networks: A taxonomic survey," *arXiv preprint arXiv:2012.15445*, 2020.
- [39] R. Ying, D. Bourgeois, J. You, M. Zitnik, and J. Leskovec, "Gnnexplainer: Generating explanations for graph neural networks," 2019.
- [40] C. Morris, N. M. Kriege, F. Bause, K. Kersting, P. Mutzel, and M. Neumann, "Tudataset: A collection of benchmark datasets for learning with graphs," in *ICML 2020 Workshop on Graph Representation Learning and Beyond (GRL+ 2020)*, 2020. [Online]. Available: www.graphlearning.io
- [41] H. Tong, B. A. Prakash, T. Eliassi-Rad, M. Faloutsos, and C. Faloutsos, "Gelling, and melting, large graphs by edge manipulation," in *Proceedings of the 21st ACM international conference on Information and knowledge management*, 2012, pp. 245–254.